Innovation, Sciences et Développement économique Canada
Office de la Propriété Intellectuelle du Canada

Innovation, Science and Economic Development Canada
Canadian Intellectual Property Office

CA 2945286 C 2023/05/09

(11)(21) 2 945 286

(12) BREVET CANADIEN
CANADIAN PATENT

(13) C

(22) Date de dépôt/Filing Date: 2016/10/12

(41) Mise à la disp. pub./Open to Public Insp.: 2017/04/13

(45) Date de délivrance/Issue Date: 2023/05/09

(30) Priorité/Priority: 2015/10/13 (US62/240,618)

(51) Cl.Int./Int.Cl. *B01D 69/00* (2006.01),
B22F 3/12 (2006.01), *C22C 5/04* (2006.01)

(72) Inventeurs/Inventors:
GAUDET, JULIE, CA;
GUAY, DANIEL, CA;
HONRADO GUERREIRO, BRUNO MANUEL, CA;
ROUE, LIONEL, CA;
TOSQUES, JACQUES, FR

(73) Propriétaire/Owner:
INSTITUT NATIONAL DE LA RECHERCHE SCIENTIFIQUE, CA

(74) Agent: LAVERY, DE BILLY, LLP

(54) Titre : METHODE ET SYSTEME DE FABRICATION DE MEMBRANES PERMEABLES A L'HYDROGENE
(54) Title: METHOD AND SYSTEM FOR FABRICATION OF HYDROGEN-PERMEABLE MEMBRANES

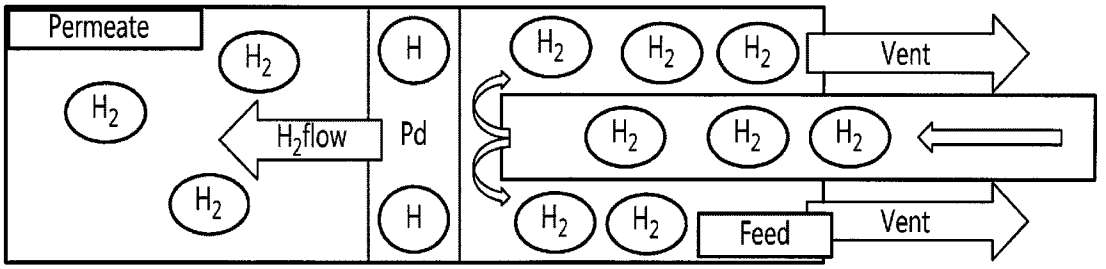

(57) Abrégé/Abstract:
A method for fabrication of an hydrogen-permeable membrane, comprising forming an alloy of a target composition and structure from powders by mechanically alloying; and forming a membrane from the alloy of the target composition and structure.

Abstract

A method for fabrication of an hydrogen-permeable membrane, comprising forming an alloy of a target composition and structure from powders by mechanically alloying; and forming a membrane from the alloy of the target composition and structure.

TITLE OF THE INVENTION

Method and system for fabrication of hydrogen-permeable membranes

FIELD OF THE INVENTION

[0001] The present invention relates to hydrogen-permeable membranes. More specifically, the present invention is concerned with a method and a system for fabrication of hydrogen-permeable membranes.

BACKGROUND OF THE INVENTION

[0002] The increasing use of hydrogen in chemical industries and oil refining and clean technologies puts pressure on hydrogen sources, hydrogen production capacities and hydrogen supplies. H_2 is used for example for fuel desulfurization, production of ammonia NH_3, methanol and other alcohol, urea, hydrochloric acid HCl, in Fischer-Tropsch reactions, i.e. conversion of CO and H_2 into liquid hydrocarbon, as a reducing agent in metallurgy and for adding value to petroleum products and oils by hydrogenation. More than 41 million tons of H_2 are produced annually, of which 80% by steam reforming, partial oxidation and auto thermal reforming of natural gas. Renewable hydrocarbons and biogas are also used as starting sources.

[0003] Methane steam reforming (see relation 1 below) is performed at high temperature, typically between about 800°C and about 900°C. The resulting H_2 and CO gas mixture is cooled down to a temperature in a range comprised between about 350°C and 450°C upon exiting a first reactor, and introduced in a second reactor where a water gas shift reaction (WGS) takes place (relation 2 below):

[0004] $CH_4 + H_2O \longrightarrow 3\ H_2 + CO$ (relation 1)

[0005] $CO + H_2O \rightleftarrows H_2 + CO_2$ (relation 2)

[0006] Then H_2 (40 mol %) is mixed with CO_2 (55 mol %), CO (3 mol %) and H_2S (1-3 mol %) from the original hydrocarbons source.

[0007] A number of methods are known to separate and purify H_2, such as: i) cryogenic

distillation, allowing a purity up to 95%, ii) separation using a polymer membrane, allowing a purity up to 98%, iii) adsorption on a molecular sieve or pressure swing adsorption (PSA), allowing a purity up to about 99.9%, and iv) separation using a metal membrane, allowing a purity of more than to about 99.95%.

[0008] In a number of applications such as in H_2 supply of fuel cells and specific files of specialized chemical industry, H_2 with a purity above 99.999% is needed. For example, fuel cells must be supplied with H_2 containing less than 100 ppm carbon monoxide or sulfur. In order to achieve such of purity levels, additional purification stages are needed after the stages of H_2 production. H_2 purification using metal membranes allow achieving high purity levels and thus look promising for such applications.

[0009] Purification by adsorption on a molecular sieve or pressure swing adsorption (PSA) is the most widely used method on production sites. In this method, each adsorbent bed goes through adsorption, depressurization, purging at low pressure and pressurization steps in a continuous operation of the pressure swing adsorption (PSA) unit. The gas flow and distribution among the beds is monitored by a complex network of valves and tubing, which makes the system delicate and the method expensive. Moreover, a dead load in the tubing and valves of the system significantly reduces the yield and efficiency of the method. Finally, the method requires cooling down the gas exiting the water gas shift (WGS) reactor from about 400°C to 40°C before going through the pressure swing adsorption (PSA) unit, which results in high energy losses.

[0010] In contrast, if the H_2 separation is done at high temperature, the purification could be integrated within the water gas shift (WGS) reactor or even within a steam reforming reactor, which would allow avoiding cooling of the gas, and therefore allow significant energy savings and method simplification.

[0011] H_2 separation at high temperature is possible using membranes that are permeable to hydrogen. In such a method, molecular H_2 at a temperature between about 450°C and 500°C is adsorbed at the surface of a membrane and dissociated into atomic H before diffusing within the membrane. Under the effect of the concentration gradient, the atomic H crosses the membrane and recombines on its opposite surface to form H_2. As the membrane is impermeable to the other species, i.e. CO, CO_2, etc., the membrane thus allows separating and purifying gas H_2 (see FIG.1).

In theory, in absence of openings in the membrane, an infinite selectivity can be achieved. H_2 separation occurs in a passive way, i.e. in absence of any mobile element, which makes the method very easy to operate and reliable. Such a method is very flexible and can easily be integrated with different types of reactors.

[0012] As hydrogen is soluble in palladium, palladium can be used for separation of hydrogen from other gases that are not soluble in palladium. However, at a high concentration of hydrogen in palladium, a phase transformation occurs which renders the membrane fragile. Moreover, Pd reacts with H_2S present in the mixture of gases being separated and forms palladium sulfildes, causing a significant drop of H_2 solubility and therefore an efficiency drop of the separation method.

[0013] In order to overcome these problems, palladium-based alloys are used with different temperatures at which H_2 causes the above-mentioned phase transformation to increase the resistance to poisoning.

[0014] There are different methods available to prepare palladium-based alloys, namely metallurgical methods (vacuum arc melting, casting), physical vapor deposition (PVD) methods (magnetron sputtering, pulse laser deposition), electrochemical and electroless deposition. Generally, metallurgical methods are used for the preparation of stand-alone membranes, while the other methods mentioned above are preferred when preparing supported membranes on porous substrates. Metallurgical methods rely on long heat treatments at high temperatures to achieve homogenous alloys. Alloys can be formed in one single step with PVD techniques, however scaling up is not straightforward. Electroless deposition consists in chemically reducing target metal salts ions that deposit on the surface of a substrate. The reduction is done in sequence, and followed by a thermal treatment to favor diffusion of the metallic ions and alloy formation. Alternatively, metallic powders of pure elements may be mixed and pressed on the substrate before applying a thermal treatment forming an alloy. In both cases, the duration and temperature of the thermal treatment are adapted according to a desired alloy composition.

[0015] There is still a need in the art for a method and system for fabrication of hydrogen-permeable membranes.

SUMMARY OF THE INVENTION

[0016] More specifically, in accordance with the present invention, there is provided a method for fabrication of an hydrogen-permeable membrane, comprising forming an alloy of a target composition and structure from powders; and forming a membrane from the alloy of the target composition and structure.

[0017] There is provided a method for fabrication of a Pd alloy hydrogen-permeable membrane, comprising forming a fcc PdCuAu ternary alloy by mechanical alloying from Pd, Cu, Au powders, promoting a phase transition from fcc to bcc by annealing; forming pellets of a resulting bcc PdCuAu alloy and cold-rolling.

[0018] Other objects, advantages and features of the present invention will become more apparent upon reading of the following non-restrictive description of specific embodiments thereof, given by way of example only with reference to the accompanying drawings.

BRIEF DESCRIPTION OF THE DRAWINGS

[0019] In the appended drawings:

[0020] FIG. 1 schematically shows separation of hydrogen by a membrane, as known in the art;

[0021] FIG. 2 is a flow chart of a method according to an embodiment of an aspect of the present invention;

[0022] FIG. 3A is a SEM photograph of BM6 70-μm aggregates;

[0023] FIG. 3B is a SEM photograph of the BM6 70-μm aggregates of FIG. 3A at a larger magnification;

[0024] FIG. 4A shows an EDX mapping of BM6 powder after ball milling : Na Kα1;

[0025] FIG. 4B shows an EDX mapping of BM6 powder after ball milling : Pd Lα1;

[0026] FIG. 5A shows a XRD graph of a powder with composition Pd41.0Cu56.1Au2.9 after ball milling;

[0027] FIG. 5B shows a XRD graph of an alloy with composition Pd41.0Cu56.1Au2.9 after first annealing;

[0028] FIG. 5C shows a XRD graph of a powder with composition Pd39.4Cu50.1Au10.1 after first ball milling;

[0029] FIG. 5D shows a XRD graph of an alloy with composition Pd39.4Cu50.1Au10.1after first annealing;

[0030] FIG. 6A is a SEM picture of BM1 pellets after final annealing;

[0031] FIG. 6B is a SEM picture of BM2 pellets after final annealing;

[0032] FIG. 6C is a SEM picture of BM4 pellets after final annealing;

[0033] FIG. 7A shows BM2 after final annealing;

[0034] FIG. 7B shows EDX mapping for BM2 of FIG. 7A: PdL;

[0035] FIG. 7C shows EDX mapping for BM2 of FIG. 7A: CuK;

[0036] FIG. 7D shows EDX mapping for BM2 of FIG. 7A: AuL;

[0037] FIG. 7E shows BM4 after final annealing;

[0038] FIG. 7F shows EDX mapping for BM4 of FIG. 7E: PdL;

[0039] FIG. 7G shows EDX mapping for BM4 of FIG. 7E: CuK;

[0040] FIG. 7H shows EDX mapping BM4 of FIG. 7E: AuL;

[0041] FIG. 8A is a SEM micrograph of a BM3 membrane before polishing;

[0042] FIG. 8B is a SEM micrograph after polishing at a first location on the surface of the membrane of FIG. 8A;

[0043] FIG. 8C is a SEM micrograph after polishing at a second location on the surface of the membrane of FIG. 8A, showing that some imperfections have remained after polishing;

[0044] FIG. 9 shows a schematic diagram of a permeation chamber for H_2 permeability measurement;

[0045] FIG. 10A shows variation of H_2 flow with time at 30, 45 and 60 psig H2 single-gas feed pressure and 464°C (pressure values on the y axis on the right side), the permeate side not submitted to any pressure control and no sweeping gas being used, measurements performed with a 277 μm membrane with composition $Pd_{40.1}Cu_{53.1}Au_{6.8}$ prepared according to the present invention;

[0046] FIG. 10B shows evolution pressure on both the retentate and permeate sides of a the membrane of Fig. 10A in function of time;

[0047] FIG. 10C shows results of an helium leak test performed on the membrane of Fig. 10A;

[0048] FIG. 11 shows a summary of single-gas permeability measurement results;

[0049] FIG. 12A shows gas mixture experiments (H_2-He 3%-941 ppm H_2S) for Pd 250 μm Alfa Aesar foil;

[0050] FIG. 12B shows gas mixture experiments (H_2-He 3%-941 ppm H_2S) for Pd pellets from commercial Pd powder;

[0051] FIG. 13A shows results of gas mixture experiments (H_2-He 3%-941 ppm H_2S) for BM1-4-:$Pd_{40.1}$ $Cu_{59.9}Au_0$;

[0052] FIG. 13B shows results of gas mixture experiments (H_2-He 3%-941 ppm H_2S) for BM15-4: $Pd_{38.8}$ $Cu_{54.5}Au_{6.6}$;

[0053] FIG. 14A shows results of gas mixture experiments (H_2-He 3%-941 ppm H_2S) for BM4-2: $Pd_{39.8}$ $Cu_{49.2}Au_{11}$;

[0054] FIG. 14B shows results of gas mixture experiments (H_2-He 3%-941 ppm H_2S) for BM4-5: $Pd_{39.8}$ $Cu_{49.2}Au_{11}$ (FIG. 14B);

[0055] FIG. 15A and FIG. 15B show EDX mapping of cross sections of the Pd 250 μm Alfa Aesar foil as commercially available membrane;

[0056] FIG. 15C, FIG. 15D and 15E show EDX mapping of cross sections of a BM3-1 - $Pd_{39.2}Cu_{53.4}Au_{7.4}$ membrane prepared according to the present invention respectively.

DESCRIPTION OF EMBODIMENTS OF THE INVENTION

[0057] FIG. 2 is a flow chart of a method according to an embodiment of an aspect of the present invention.

[0058] First PdCuAu ternary alloys (fcc) are formed by mechanical alloying from Pd, Cu, Au and NaCl (2 wt%) powders (step 12). A phase transition from fcc to bcc is promoted by annealing the PdCuAu alloy at 400°C for 5h under a mixture of Ar/5%H_2 (step 14). Then pellets are formed by pressing 300 mg of bcc PdCuAu alloy into a 1.1 cm disk with a thickness of approximately 450 μm using a load of 20 metric tons for 10 min in a hydraulic press (step 16). The resulting pellets are then sintered at 900°C for 1h under a mixture of Ar/5% H_2 (step 18), and then the surface of the pellets are homogenized by cold-rolling with a distance between rolls starting at 500 μm and decreased by steps of 25 μm (step 20). A final annealing is performed at 400°C for 5h under a mixture of Ar/5%H_2 (step 22), before polishing the pellets (step 24) to obtain an almost-mirror finish like surface.

[0059] Pd pellets are heat treated under pure Ar only (steps 14, 18 and 22) to avoid the formation of cracks during cool down.

[0060] Membranes thus obtained were tested under single gas conditions, first with He and then with H_2; a final He leak test was further performed. Membranes were considered leak free, meaning that no gas was permeating through defects or pinholes, when no flow was registered in the helium tests, i.e. flow below 0.005 ml/min, which was the resolution limit.

[0061] In step 12, Pd, Cu and Au powders were ball milled for at least 10 hours, i.e. for example18h under Ar. NaCl was used as a process control agent. One stainless steel ball of 2 g and 2 stainless steel balls of 1 g were used. All solids were weighted and sealed under Ar. Ball milling was performed with no temperature control. Amounts of Pd, Cu, Au and NaCl used in 5 different compositions BM_{1-5} are listed in Table 1 below:

Synthesis	Pd (g)	Cu (g)	Au (g)	NaCl (g)	Total solids (g)
BM1	1.034	0.926	0.000	0.04	2
BM2	0.985	0.838	0.137	0.04	2
BM3-BM5	0.927	0.733	0.300	0.04	2
BM4	0.875	0.640	0.445	0.04	2

Table 1

[0062] As can be seen by X-ray diffraction (XRD), ball milling promotes the formation of one single fcc PdCuAu alloy; in some cases, unalloyed metals can still be identified in the diffractograms (see Table 2 below). However, subsequent heat treatments guarantee complete alloying at all compositions (see Table 3 below).

	Pd (at%)	Cu (at%)	Au (at%)	Impurities*	XRD
BM1	39.2	60.8	0.0	NaCl/Fe,Ni	fcc
BM2	41.0	56.1	2.9	NaCl/Fe	fcc+Pd+Cu
BM3	39.8	52.7	7.5	NaCl	fcc
BM4	39.4	50.5	10.1	NaCl/Fe	fcc+Pd+Cu+(Au)
BM6	95	---	---	5 at% Na	Pd

Table 2

[0063] As can be seen in the electron microscopy (SEM) photographs of FIGs. 3 representative of the aggregates of BM1-BM6, aggregates 70μm and below are obtained. The composition of the alloys does not seem to have an effect on the size or shape of the aggregates.

[0064] Element distribution images (EDX) of BM6 powder after ball milling shown in FIGs. 4 suggest that NaCl is dispersed on the surface of palladium forming granules 2 μm long.

[0065] In step 14, heat treatment is performed at 400°C under Ar 5%H2 for 5 hours. Complete transition from fcc to bcc phase may occur depending on the alloy composition. Unalloyed metals are no longer observed in XRD (see FIGs. 5 and Table 3 below).

	Pd (at%)	Cu (at%)	Au (at%)	XRD after 1st HT
BM1	39.2	60.8	0.0	bcc
BM2	41.0	56.1	2.9	bcc
BM3	39.8	52.7	7.5	bcc
BM4	39.4	50.5	10.1	fcc+bcc

Table 3

[0066] In step 16, 300 mg of bcc PdCuAu alloy was pressed into a 1.1 cm disk and about 450 μm thick using 20 metric tons for 10 min.

[0067] In step 18, the resulting pellets were sintered at 900°C for 1h under a mixture of Ar/5%H_2.

[0068] In step 20, the thickness of the pellets was decreased and homogenized by cold rolling, with a distance between rolls starting at 500 μm and decreased by steps of 25 μm.

[0069] Table 4 below shows measurements taken on different days before and after cold rolling. Only the results of membranes that showed 0 ml/min flow under He are shown.

	Thickness (um)	
Membrane	Before CR	After CR*
BM1-2	477	362
BM2-2	449	354; 359#
BM4-2	421	307; 319#
BM5-2	548	440

Table 4

[0070] In step 22, the membranes were annealed at 400°C for 5h under Ar/5%H_2. SEM, EDX composition and XRD analysis were performed. Fe content was found to be below 1 at%; there was no clear evidence for the presence of NaCl (see Table 5 below and FIGs. 6).

	Pd (at%)	Cu (at%)	Au (at%)	XRD after 2nd annealing
BM1	40	60	0.0	Bcc
BM2	40	57	3	Bcc
BM3	39	53	7	bcc(+fcc??)
BM4	40	49	11	bcc+fcc
BM5	39	54	7	bcc

Table 5

[0071] FIGs. 7 shows EDX mapping after final annealing. EDX mapping shows homogenous distribution of all 3 elements Pd, Cu and Au throughout the membrane (Images taken at 2500 times magnification).

[0072] In step 24, all membranes were polished using SiC sanding paper (P800 – P1500 – P2500). Polishing was finished with Al_2O_3 1μm paste on a microcloth. Both sides of the membranes were polished. It was found that polishing decreases defects and pinholes on the surface of the membranes, making the membranes more selective. For example, the flow under 60 psig He may be reduced from 0.80 ml/min to less than 0.005 ml/min (detection limit of He mass flow meter) by polishing (see FIGs. 8). Diamond paste (6 μm and 1 μm) was used instead of SiC sanding paper P2500 and Al_2O_3, when polishing pure Pd pellets.

[0073] Table 6 below shows the thickness in μm of the membranes obtained after polishing:

Membrane #	After polishing (um)
BM1-2	327
BM2-2	300
BM4-2	304
BM5-2	277

Table 6

[0074] Then H_2 permeability was measured, using the configuration of a permeation chamber as shown in FIG. 9, operated in dynamic mode, i.e. with a constant flow of gas in the feed

side (excess is vented to exit), at a temperature of about 350-450°C (from furnace display), a pressure on feed side below 100 psig (7.8 atm), 3 MF (H_2 0-100 ml/min; H_2 0-20 ml/min; He 0-5 ml/min; detection limit of He MF: 0.005 ml/min); 2 pressure gauges (feed/permeate).

[0075] FIGs. 10 show single gas experiments for BM5-2, of a composition of $Pd_{40.1}Cu_{53.1}Au_{6.8}$. This membrane failed the initial He leak test, but was successfully repaired by cold rolling, annealing and polishing. Final thickness was 277 μm. The membrane was assembled in the permeation chamber between two stainless steel gaskets for support. The chamber was subsequently degassed by alternating three times 5 min vacuum with 30 psig Ar. Afterwards the temperature was raised to 50°C while keeping Ar inside the furnace at atmospheric pressure. Finally, 10 psig H_2 was introduced and the temperature was raised to 450°C.

[0076] Ideal selectivity is used when operating with single gases as:

$$\alpha^{*}_{H2/He} = \frac{Permeability_{H2}}{Permeability_{He}}$$

[0077] The separation factor for gases in mixtures, also called the selectivity of the membrane, $\alpha_{H_2,j}$, is given by the mole fractions of the components in the feed (x) and in the permeate (y):

$$\alpha_{H_2,j} = \frac{y_{H_2}/y_j}{x_{H_2}/x_j}$$

G1 (psig)	G2 (psig)	Flow (ml/min)	Permeability ($mol.m^{-1}.s^{-1}.Pa^{-0.5}$)	α*
He 57.7	-1.17 (ΔP=-0.3)	<0.005	$<5.0\times10^{-11}$	
29.32	-0.33	0.89	2.3×10^{-8} (R^2=0.9980)	>469
43.16	-0.34	1.39		
59.06	-0.33	1.82		
He 58.48	-1.08 (ΔP=-0.28)	<0.005	4.9×10^{-11}	

Table 7

[0078] Table 7 gives the data of each point of FIGs. 10.

[0079] FIG. 11 shows a summary of single-gas permeability measurement results (circles), with a pressure on retentate of 30-60 psig and permeate at atmospheric pressure. Results by McKinley (US patent 3 439 474 – 1969) are also shown (squares), for measurements performed on 25.4 μm foils supported on porous stainless steel substrates, and permeate at atmospheric pressure.

[0080] FIGs. 12 show results of gas mixture experiments (H_2-He 3%-941 ppm H_2S) for a Pd 250 μm Alfa Aesar foil membrane as commercially available (FIG. 12A) and for Pd pellet from a commercial Pd powder (FIG. 12B). In the first case (FIG. 12A), a 50% decrease in permeability was observed at time 60 min in the presence of H_2S 941 ppm and switching to pure H_2 at time 90 min allowed a recovery of 70% of the initial permeability; no He was detected downstream. In the second case (FIG. 12B), a 47% decrease in permeability was observed in the presence of H_2S 941 ppm at time 30 min; and switching to pure H_2 at time 60 min allowed a complete recovery to the initial permeability with a final selectivity α=27.6.

[0081] FIGs. 13 show results of gas mixture experiments (H_2-He 3%-941 ppm H_2S) for BM1-4: $Pd_{40.1}Cu_{59.9}Au_0$ (FIG. 13A), and for BM5-4: $Pd_{38.8}Cu_{54.5}Au_{6.6}$ (FIG. 13B). In the first case (FIG. 13A), a 12% decrease in permeability was observed at time 30 min in the presence of H_2S 941 ppm

and the membrane ruptured at the end. In the second case (FIG. 13B), a 74% decrease in permeability was observed in the presence of H_2S 941 ppm at time 30 min and switching to pure H_2 at time 60 min allowed a 58% recovery to the initial permeability with a final selectivity α=1.

[0082] FIGs. 14 show results of gas mixture experiments (H_2-He 3%-941 ppm H_2S) for BM4-2: $Pd_{39.8}Cu_{49.2}Au_{11}$ (FIG. 14A) and for BM4-5: $Pd_{39.8}Cu_{49.2}Au_{11}$ (FIG. 14B). In the first case (FIG. 14A), a 75% decrease in permeability was observed at time 30 min in the presence of H_2S 941 ppm and switching to pure H_2 at time 60 min allowed a 55% recovery to the initial permeability. In the second case (FIG. 14B), a 48% decrease in permeability was observed in the presence of H_2S 941 ppm and switching to pure H_2 allowed a 71% recovery to the initial permeability with a final selectivity α=1.9.

[0083] FIGs.15 show EDX mapping of cross sections of the Pd 250 μm Alfa Aesar foil membrane as commercially available (FIGs. 15A, 15B) and of a BM3-1 - $Pd_{39.2}Cu_{53.4}Au_{7.4}$ membranes prepared according to the present invention respectively (FIGs.15C-15E), all being heat treated with H_2S for 15 min at 450°C.

[0084] In the case of Alfa Aesar foil membrane as commercially available, FIGs. 15A and 15B show an homogeneous distribution of Pd (FIG. 15A) and S (FIG. 15B) within the bulk of the membrane, which may compromise the efficiency of the membrane for separating hydrogen.

[0085] In the case of the $Pd_{39.2}Cu_{53.4}Au_{7.4}$ membrane prepared according to the present invention, FIGs. 15D and 15E respectively show that Cu and S segregate on the surface of the membrane. As such, these surface elements may be removed by cleaning of the membrane; with only less than about 10% of the elements Cu or S being found in the bulk of the membrane, the membrane may still be efficient for separating hydrogen.

[0086] There is thus provided a method for the production of H_2 permeable membranes from ball milled powders. The method allows producing membranes of a thickness comprised in a range between 277 μm and 327 μm.

[0087] Four different compositions of PdCuAu alloys were tested. About 4 compositions in 10 were found to pass initial leak tests (pellets of PdCuAu alloys).

[0088] Tests performed using Pd-Cu, Pd-Cu-Ag and Pd-Cu-Au showed that the membranes obtained had a composition very similar to the powder initially used to form the alloy after milling. This allows controlling the composition of the membrane by controlling the composition of the initial powder mixture. Membranes with composition Pd40Cu(60-x)Aux with x=0, 3, 7 and 11at% were formed.

[0089] A last polishing step was found to allow obtaining highly hydrogen selective membranes; it was shown that membranes that developed leaks during testing could be regenerated by polishing. Selectivity of the membranes under pure hydrogen conditions, called ideal selectivity, was higher than 130; after re-polishing a selectivity higher than 469 was obtained. Selectivity in the presence of H_2S is below 28.

[0090] The lowest He flow that was possible to measure was 0.005 ml/min. This corresponds to a permeability of He below 5×10^{-9} $mol.m^{-1}.s^{-1}.Pa^{-0.5}$. Consequently, ideal selectivity factors are above 130. Preliminary gas chromatography (GC) measurements showed that 6 ppmv He is present in the permeate side of a membrane prepared from commercial Pd powder after 15 min under 45psig He. Comparatively, a commercial Pd 250 µm foil shows under the same conditions a He content below 1 ppmv. Obtained hydrogen permeability, under pure hydrogen gas conditions, varied between 6.9×10^{-9} $mol\ m^{-1}s^{-1}Pa^{-0.5}$ and 2.1×10^{-8} $mol\ m^{-1}s^{-1}Pa^{-0.5}$.

[0091] The selectivity considerably decreases in the presence of H_2S; the longer the time of exposure to H_2S gas mixture, the lower the selectivity. This is specific to the PdCuAu alloys and to the experimental conditions (temperature, pressure and H_2S concentration) and is not related to the method used to prepare the membranes.

[0092] In the presence of pure H_2S, copper, and possibly gold, segregate to the surface. This creates a layer that binds to sulfur preventing it from fully migrating to the bulk of the membrane, as it happens with pure Pd. The higher the Au content of the membrane, the lower the S content in the bulk. As the S-contaminants remain mostly on the surface, a cleaning method may be designed to recover the initial activity of the membrane.

[0093] However, the Cu-S-and possibly Au layer on top of the membrane may prevent H_2 permeation.

[0094] The present method comprises formation of an alloy of a target composition and structure directly from mechanically alloying the precursor powders using ball milling technique. More precisely, the method comprises pressing and sintering the obtained powder, before cold-rolling and polishing.

[0095] Cold spray, colloidal spray or paste painting may also be contemplated to prepare membranes supported on porous substrates from the mechanically alloyed powders.

[0096] The present alloy preparation method, being an out of equilibrium method, allows fabricating membranes with compositions that cannot be reached using conventional methods, such as membranes in metastable alloys, extended solid solution etc..., which in turn allows tailoring specific membrane shaving target properties, in terms of H_2 permeability for example.

[0097] Large quantities of powder may be prepared simultaneously, depending on the size of the crusher used, which may have a capacity of up to Kg in industrial settings.

[0098] There is generally provided a method for preparation of palladium alloys from powders by mechanical alloying. There is provided a method for fabrication of hydrogen-permeable membranes from alloy powders produced by ball milling.

[0099] The scope of the claims should not be limited by the embodiments set forth in the examples, but should be given the broadest interpretation consistent with the description as a whole.

Claims

1. A method for fabrication of an hydrogen-permeable membrane, comprising:

a) forming an alloy of a target composition and structure from powders; and

b) forming a membrane from the alloy of the target composition and structure.

2. The method of claim 1, wherein said step a) comprises mechanically alloying the powders.

3. The method of claim 1, wherein said step a) comprises mechanically alloying the powders and annealing the alloy.

4. The method of claim 1, said step a) comprises ball milling the powders.

5. The method of claim 1, said step a) comprises ball milling the powders and heat treatment.

6. The method of any one of claims 1 to 5, wherein said step b) comprises forming the membrane by cold rolling.

7. The method of any one of claims 1 to 5, wherein said step b) comprises forming the membrane by one of: cold spraying, colloidal spraying and paste painting the alloy of the target composition and structure on a substrate.

8. The method of any one of claims 1 to 7, for fabrication of a Pd alloy hydrogen-permeable membrane, said step a) comprising mechanically alloying Pd with at least one of Cu, Au and Ag powders.

9. The method of any one of claims 1 to 8, wherein said step a) comprises mechanically alloying Pd, Cu, and Au powders into a fcc PdCuAu alloy and annealing into a bcc PdCuAu alloy.

10. The method of any one of claims 1 to 6, for fabrication of a PdCuAu alloy hydrogen-permeable membrane, said step a) comprising mechanically alloying at least Pd and Cu, and Au powders into a fcc PdCuAu ternary alloy and annealing into a bcc PdCuAu ternary alloy, said step b) comprising cold rolling pellets of the bcc PdCuAu ternary alloy.

Date Reçue/Date Received 2022-06-16

11. The method of any one of claims 1 to 10, further comprising at least one of annealing the membrane and polishing the membrane.

12. The method of any one of claims 1 to 6, further comprising annealing and polishing the membrane.

13. A method for fabrication of a Pd alloy hydrogen-permeable membrane, comprising forming a fcc PdCuAu ternary alloy by mechanical alloying from Pd, Cu, Au powders, promoting a phase transition from fcc to bcc by annealing; forming pellets of a resulting bcc PdCuAu alloy and cold-rolling.

14. The method of claim 13, further comprising polishing.

Date Reçue/Date Received 2022-06-16

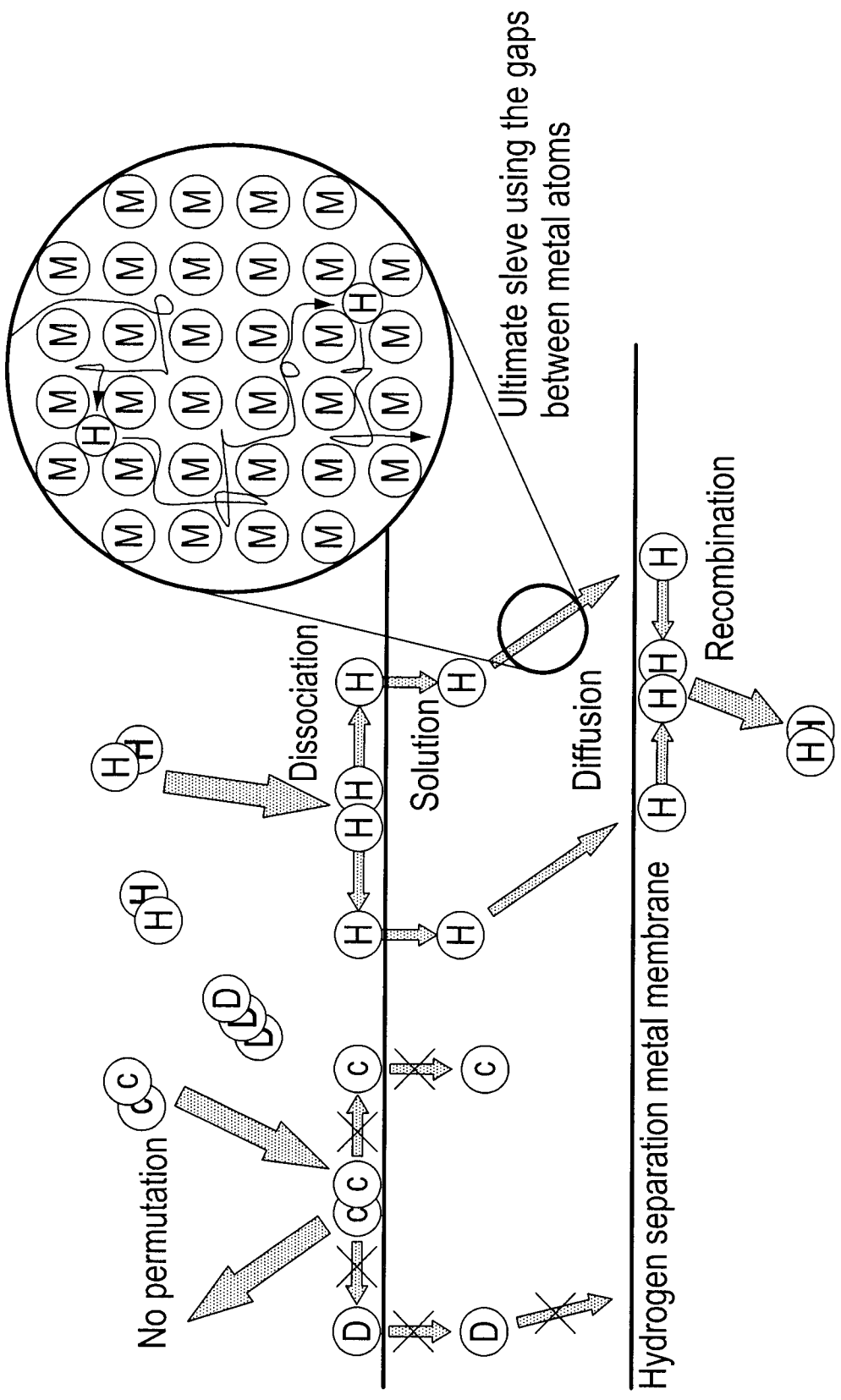

Fig. 1 (PRIOR ART)

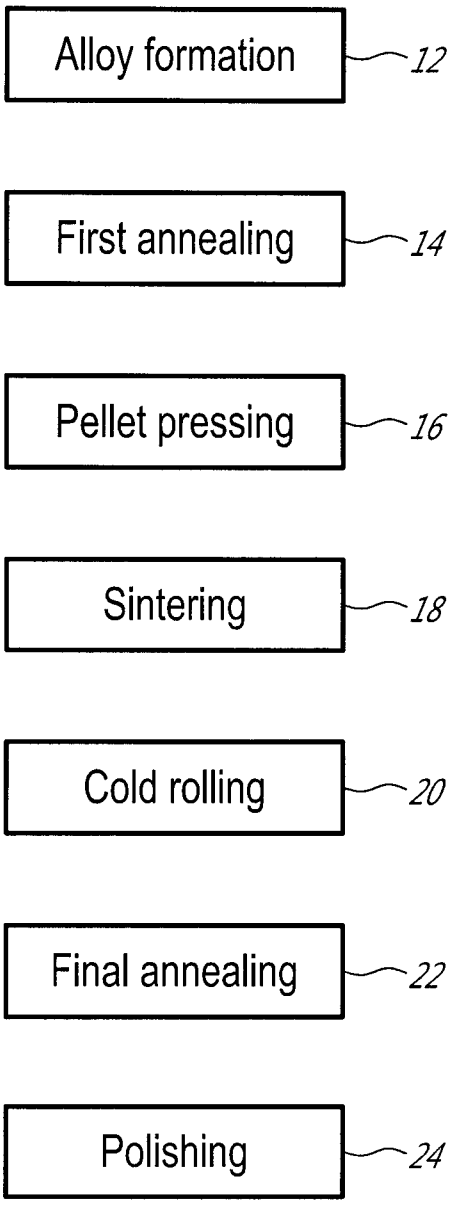
Alloy formation
12
First annealing
14
Pellet pressing
16
Sintering
18
Cold rolling
20
Final annealing
22
Polishing
24

Fig. 2

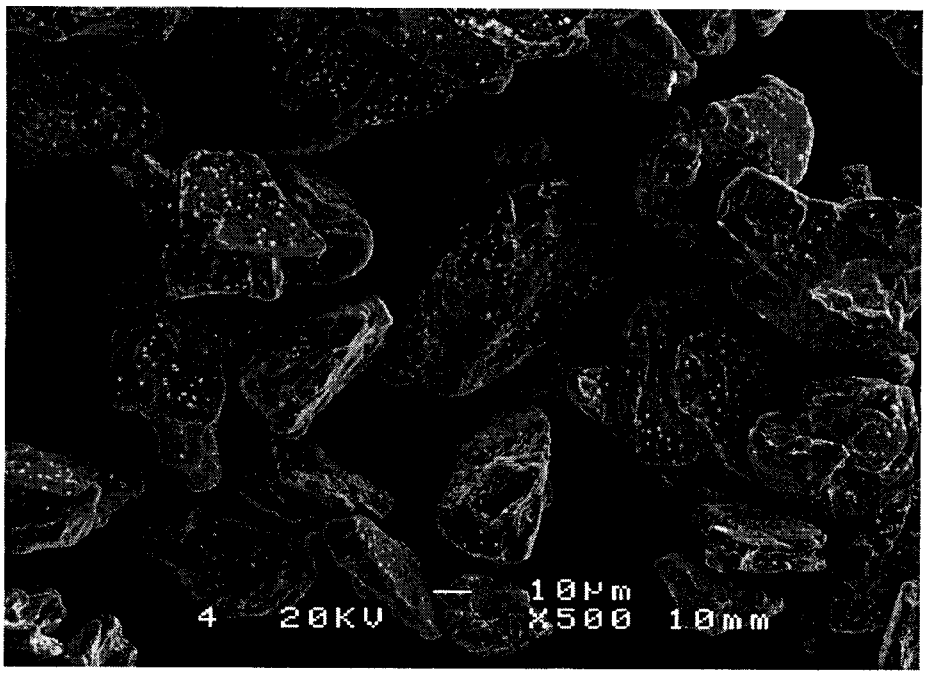

FIG. 3A

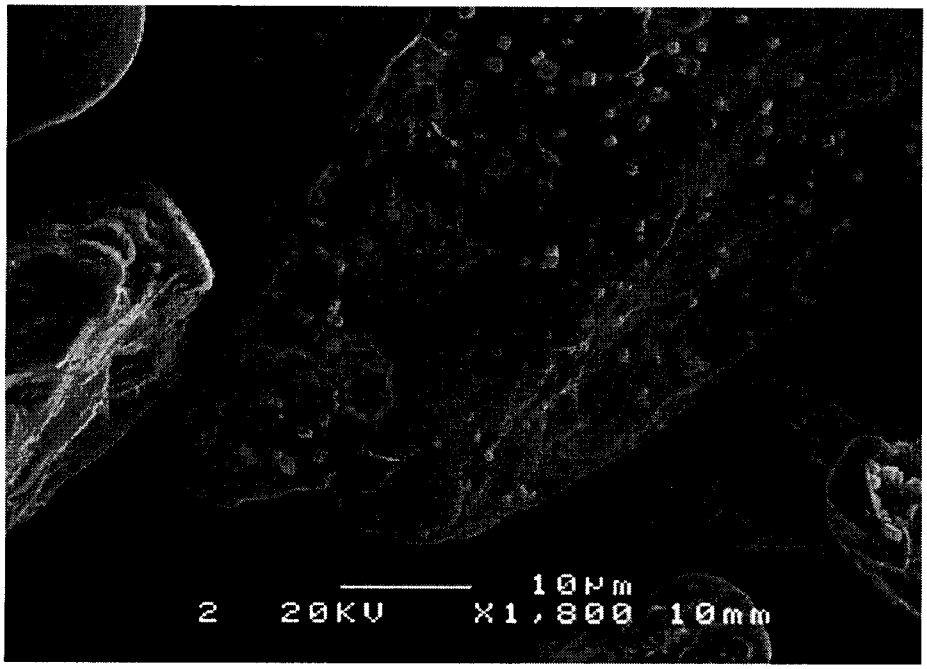

FIG. 3B

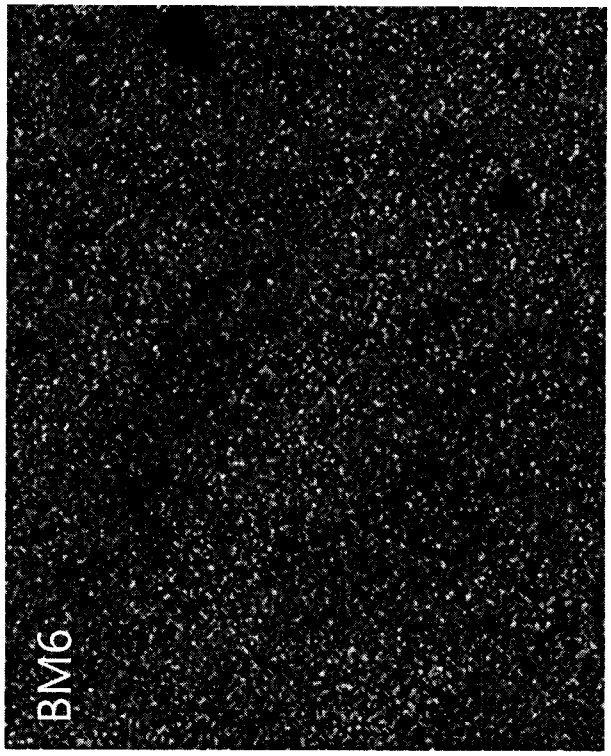

Pd Lα1

Fig - 4B

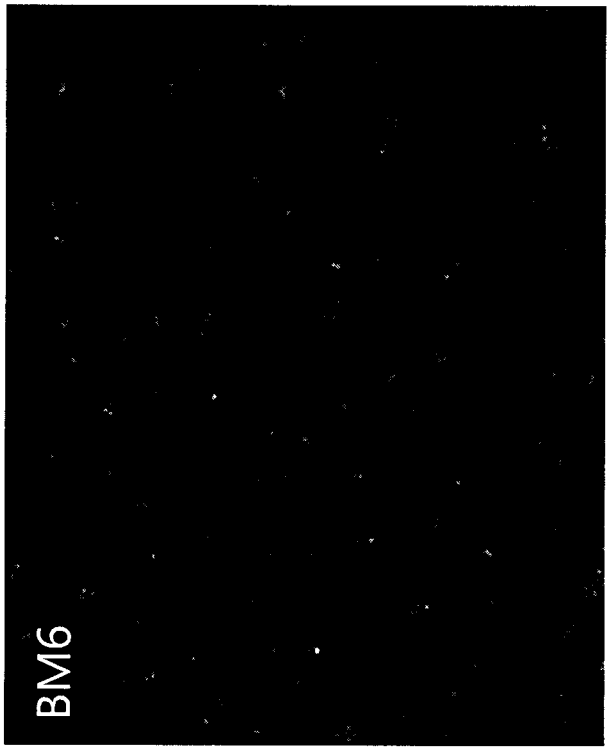

Na Kα1

Fig - 4A

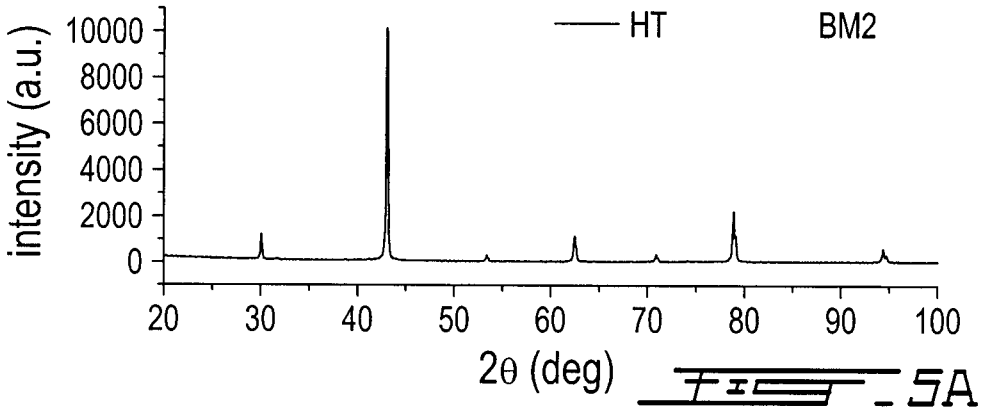

Fig. 5A

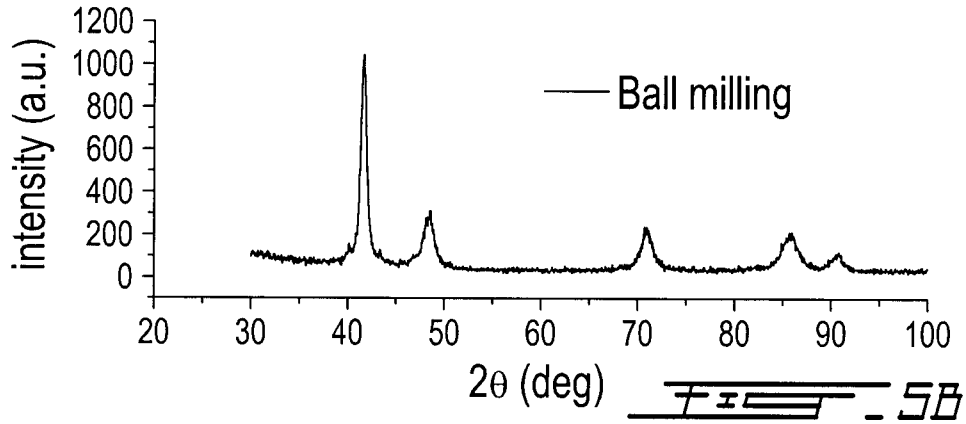

Fig. 5B

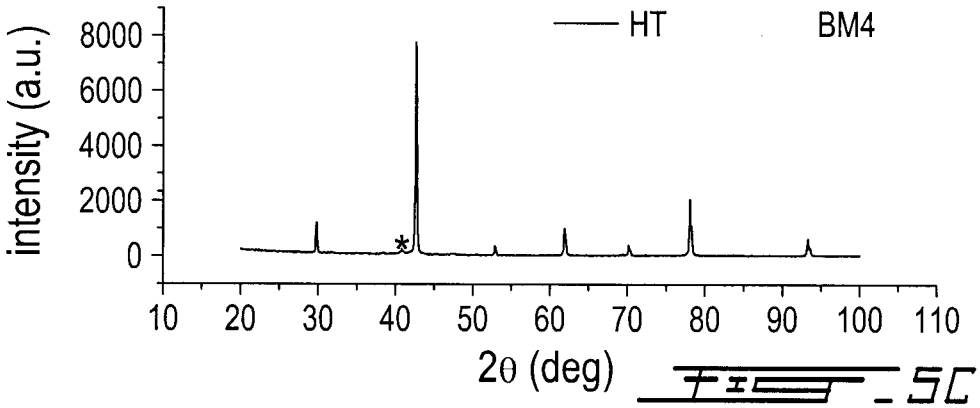

Fig. 5C

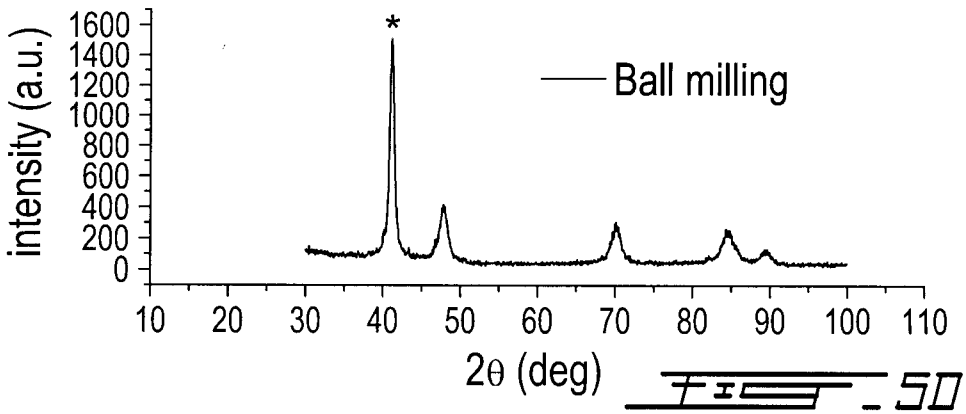

Fig. 5D

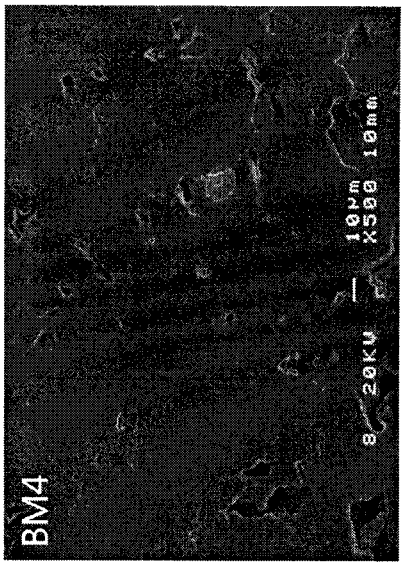

Fig. 6C

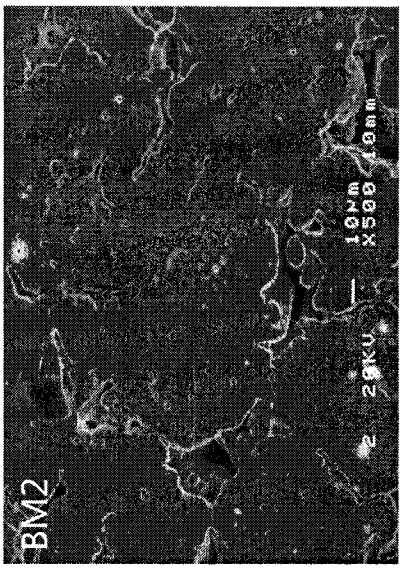

Fig. 6B

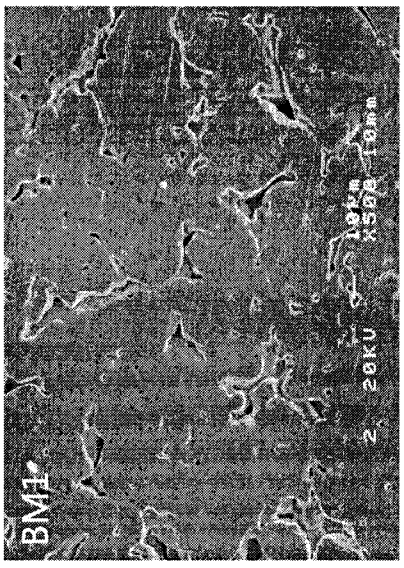

Fig. 6A

Fig. 7A Fig. 7B Fig. 7C Fig. 7D

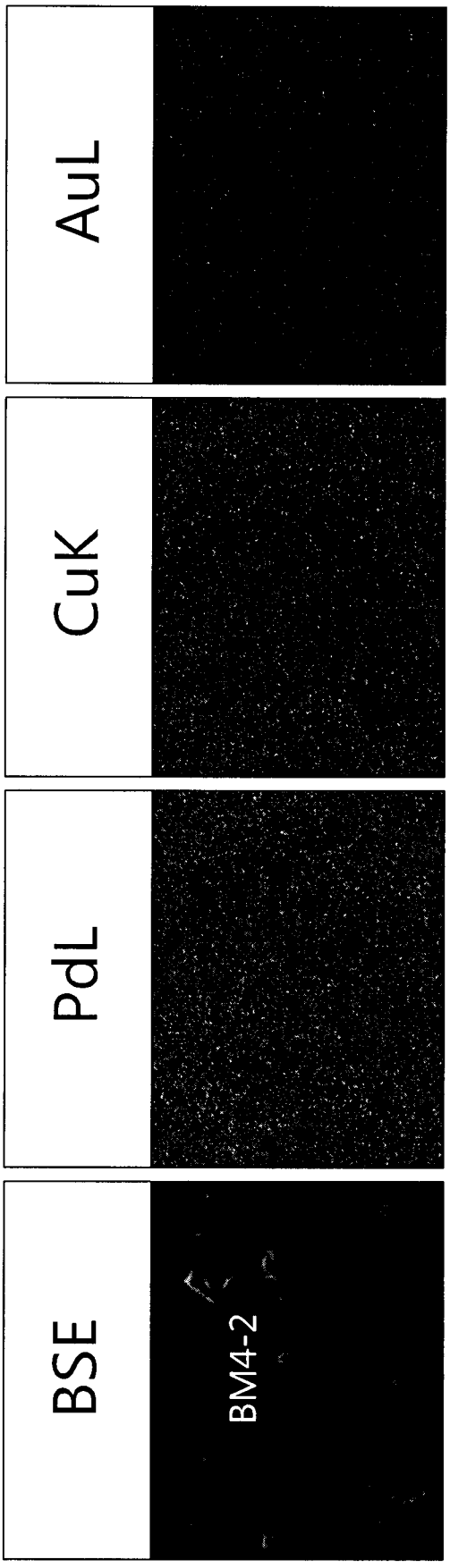

Fig. 7E Fig. 7F Fig. 7G Fig. 7H

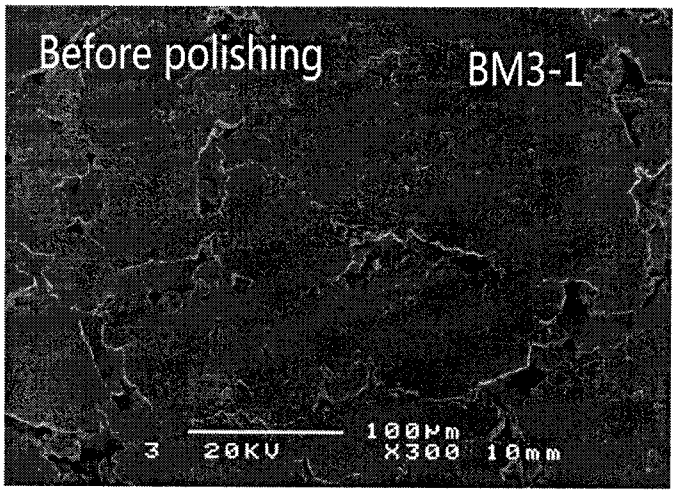

FIG. 8A

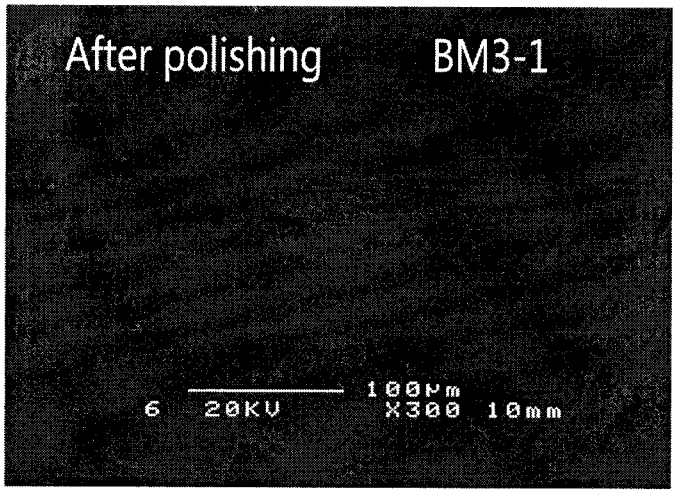

FIG. 8B

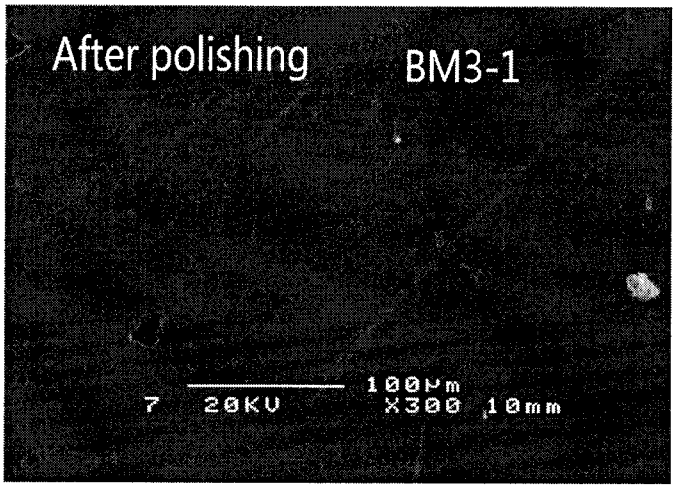

FIG. 8C

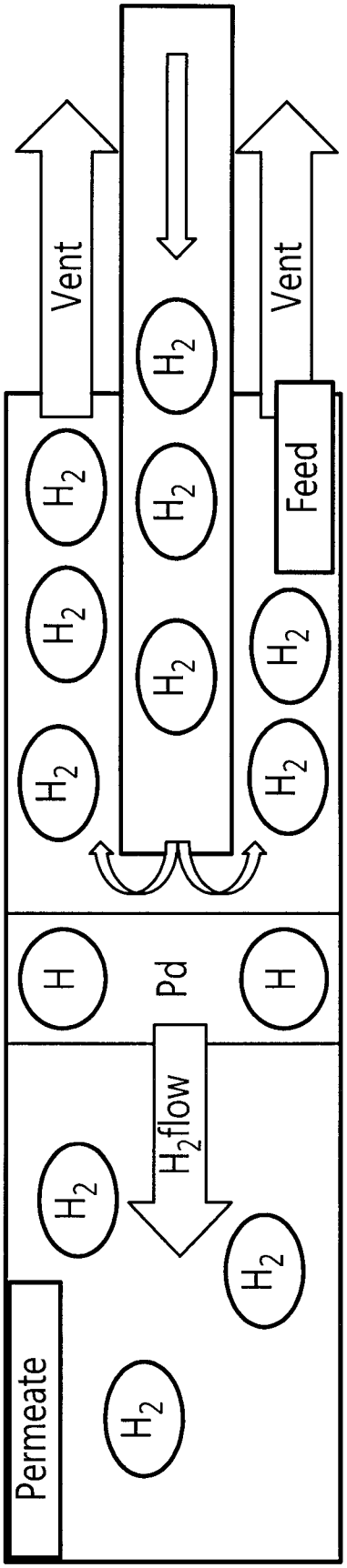

Fig. 9

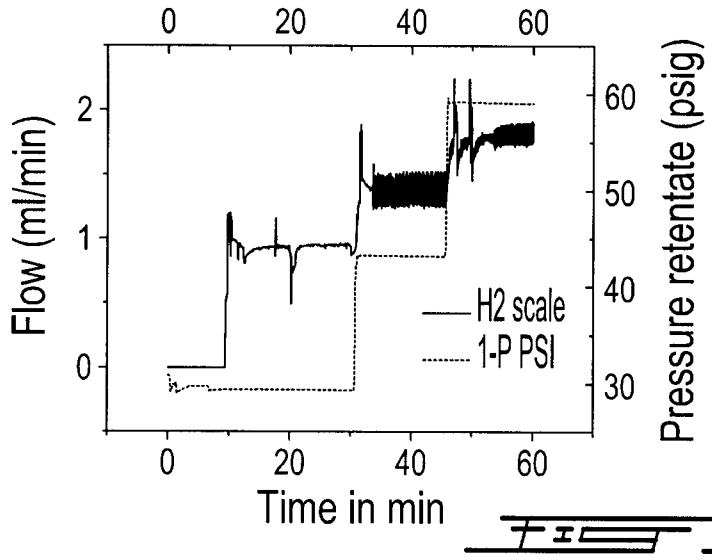

Fig. 10A

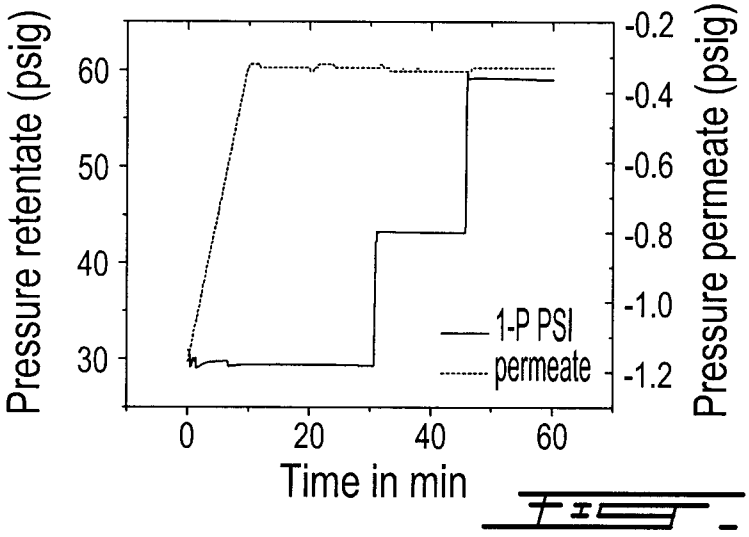

Fig. 10B

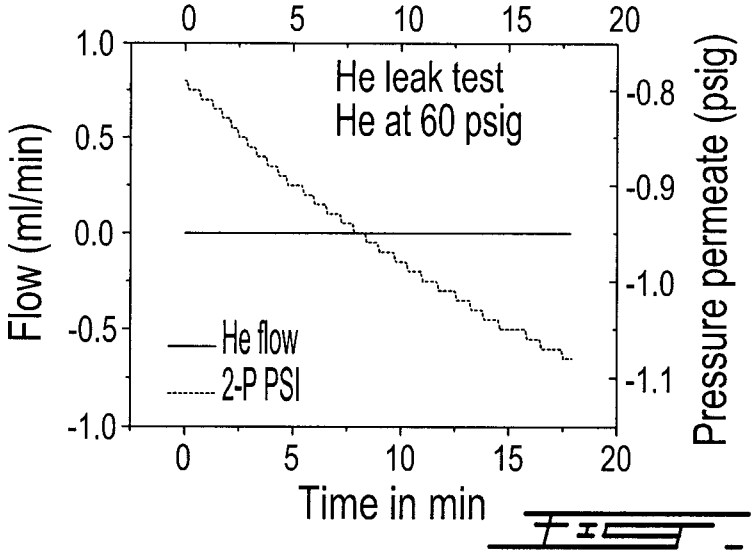

Fig. 10C

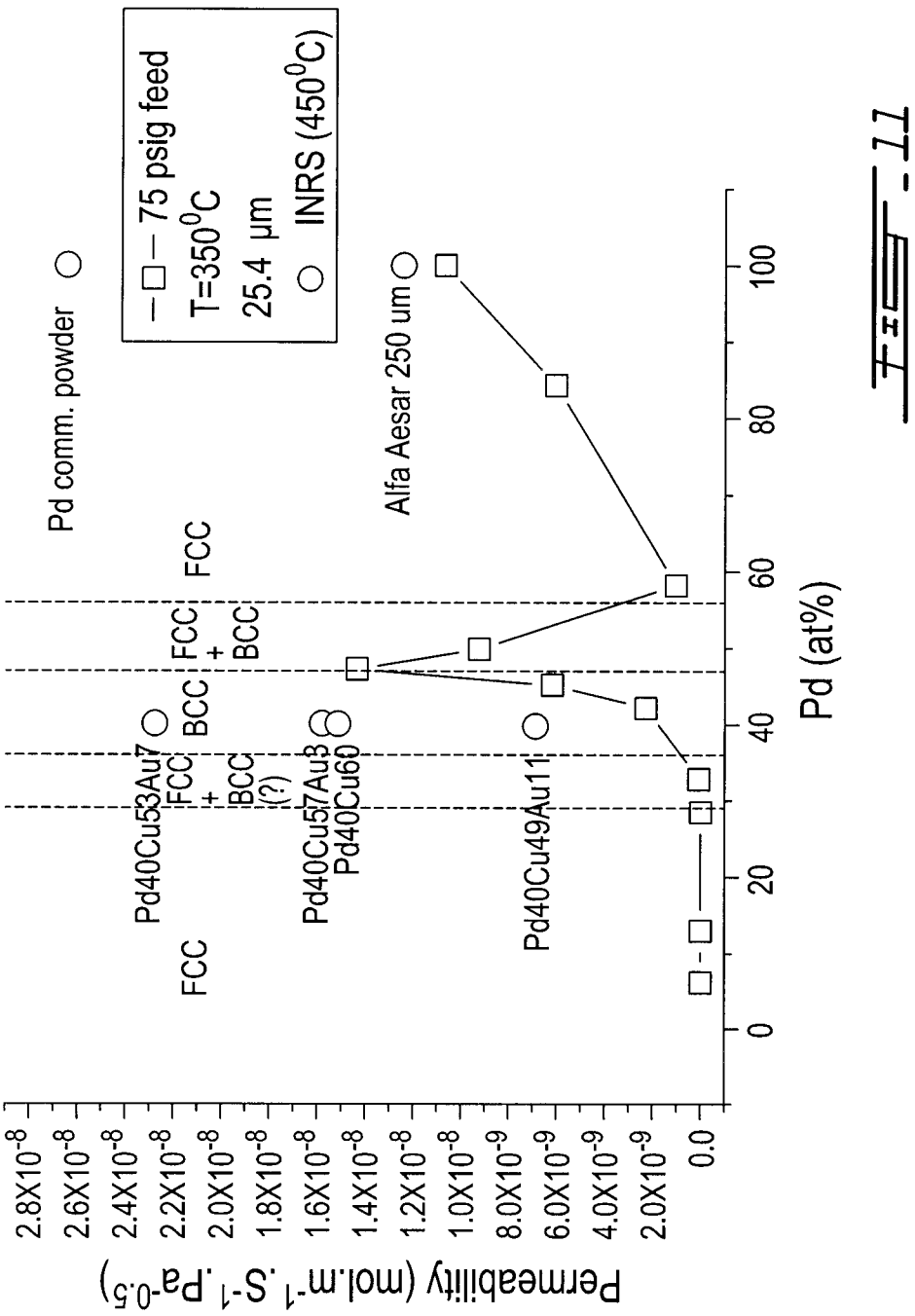
Permeability (mol.m-1.S-1.Pa-0.5)
2.8X10-8
2.6X10-8
2.4X10-8
2.2X10-8
2.0X10-8
1.8X10-8
1.6X10-8
1.4X10-8
1.2X10-8
1.0X10-8
8.0X10-9
6.0X10-9
4.0X10-9
2.0X10-9
0.0
0
20
40
60
80
100
Pd (at%)
Pd comm. powder
75 psig feed
T=350°C
25.4 µm
INRS (450°C)
Alfa Aesar 250 um
Pd40Cu53Au7
FCC
Pd40Cu57Au3
FCC + BCC (?)
Pd40Cu60
FCC + BCC
FCC
Pd40Cu49Au11
FCC

Fig - 11

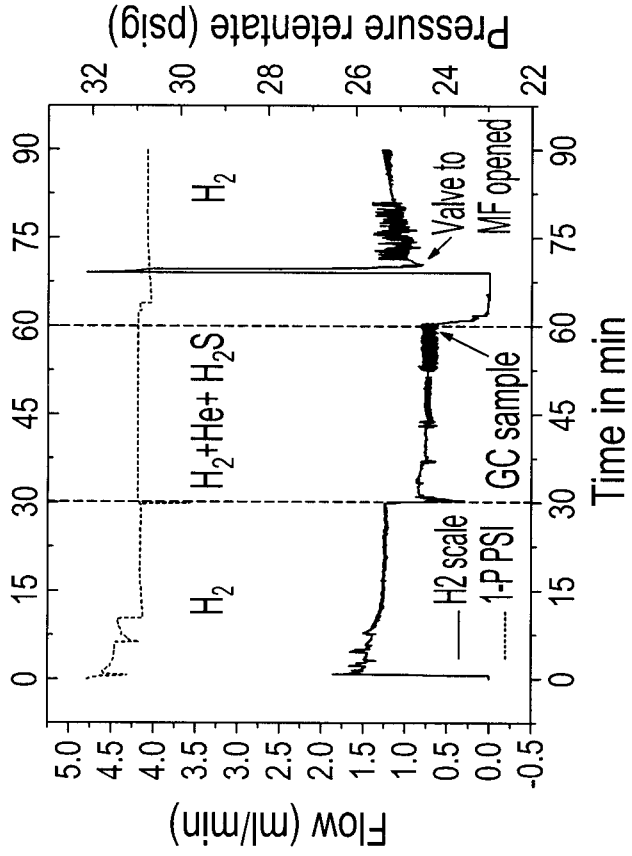

FIG - 12B

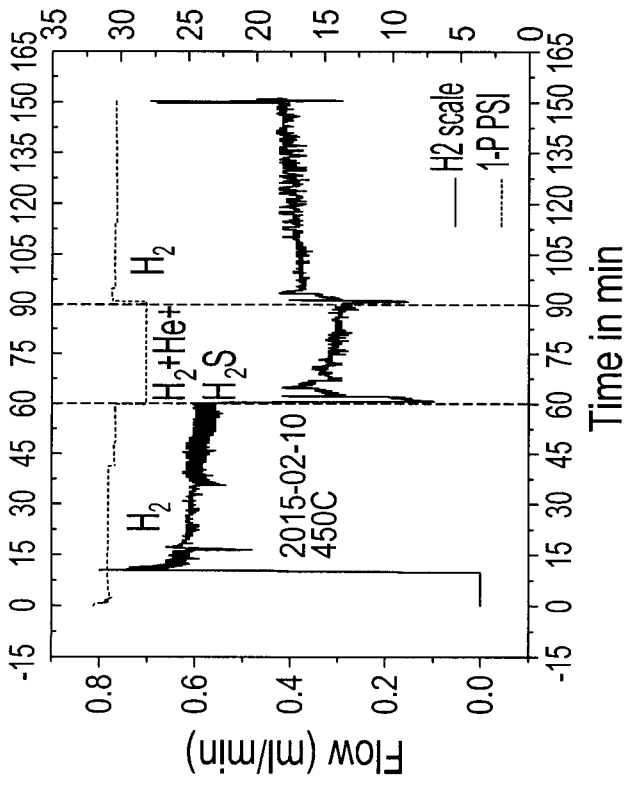

FIG - 12A

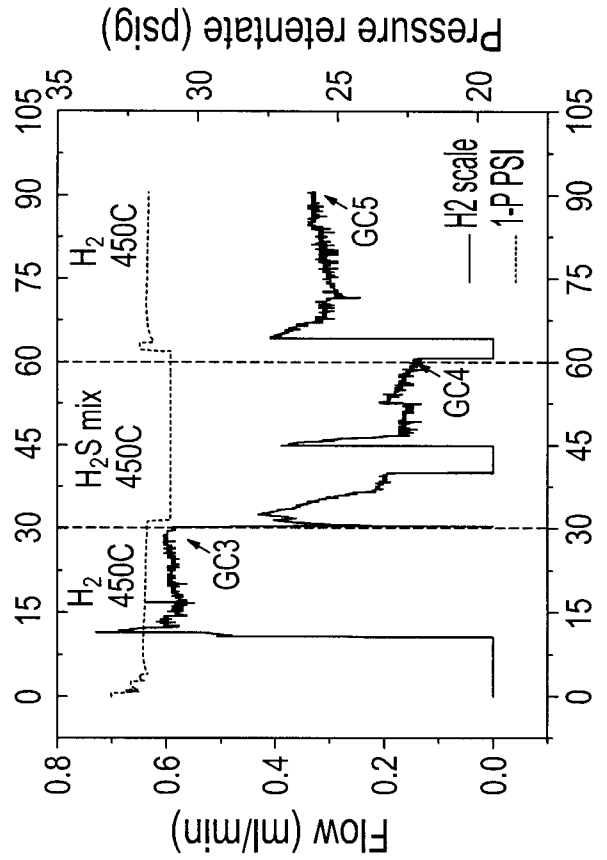

FIG-13B

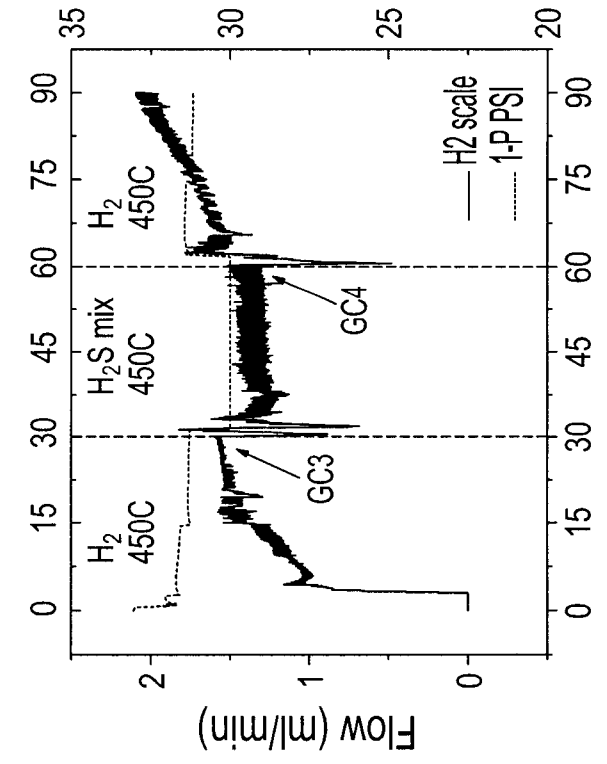

FIG-13A

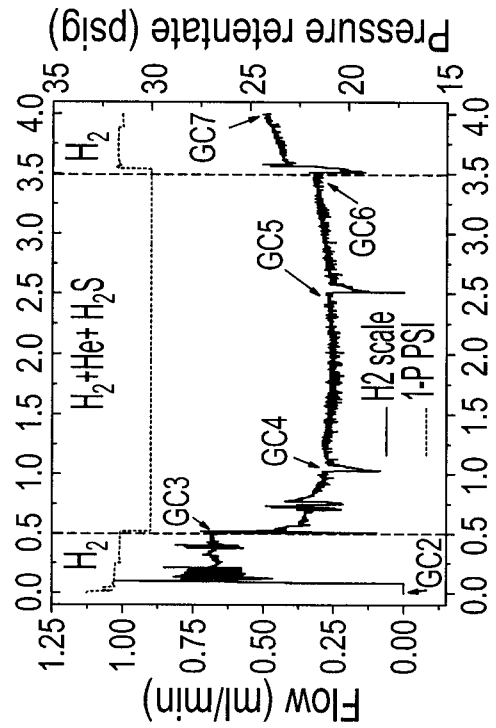

GC	α
4	4.3
5	2.6
6	1.9

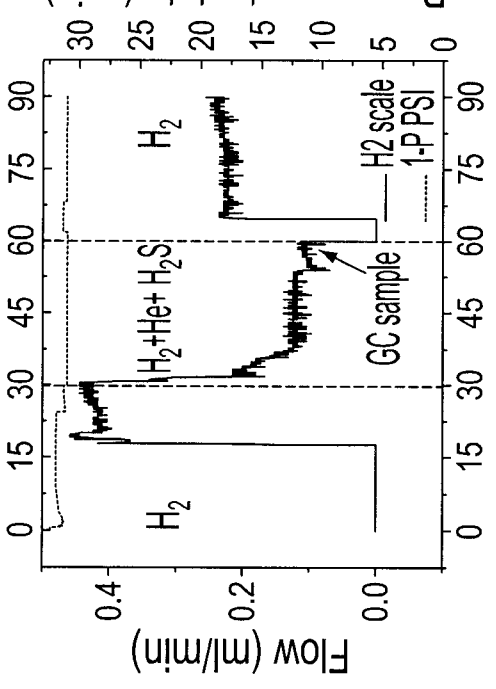

FIG -14A

FIG -14B

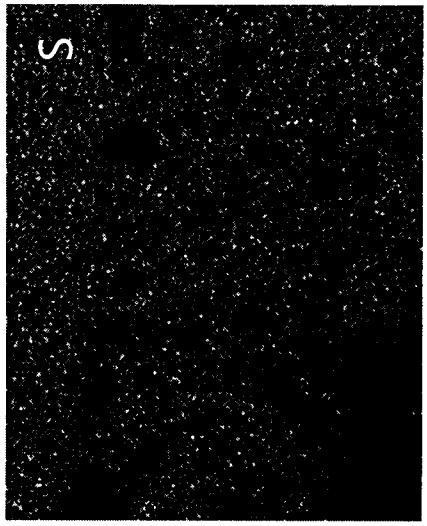

Fig-15B

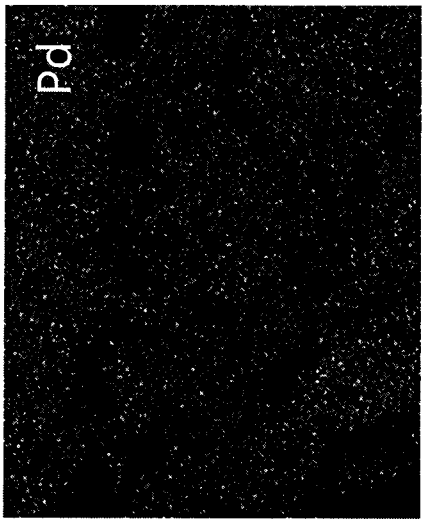

Fig-15A

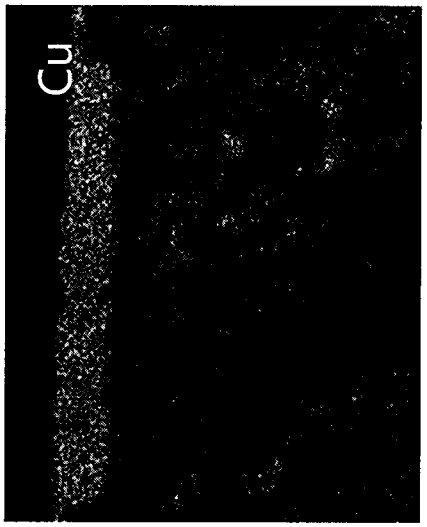

Fig-15D

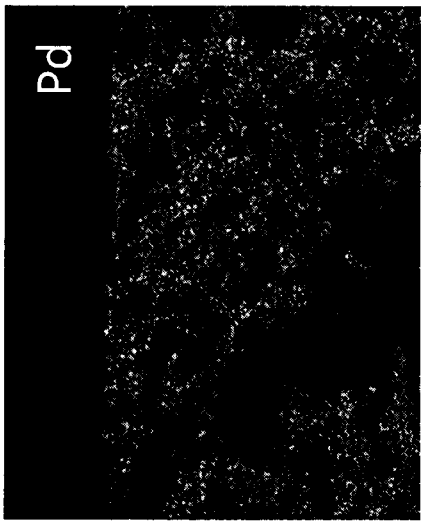

Fig-15C

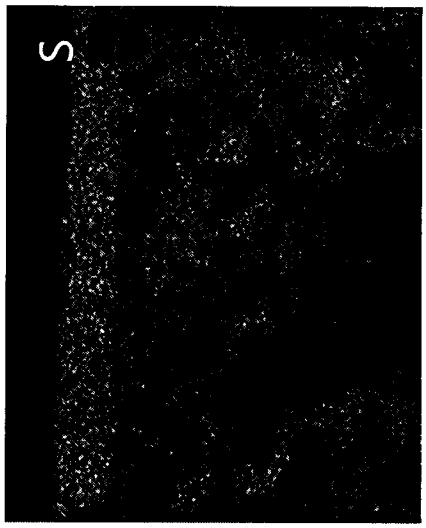

Fig-15E

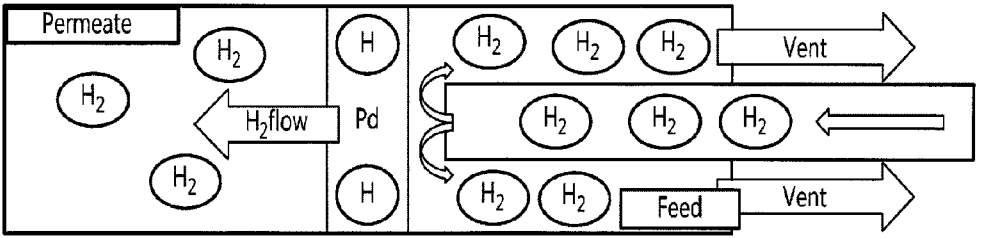
Permeate
H2
H2
H2flow
H2
H
Pd
H
H2
H2
H2
Vent
H2
H2
H2
H2
H2
Feed
Vent